AFCRL-69-0259

STUDY OF RADIATION EFFECTS ON NOVEL SEMICONDUCTOR DEVICES

by

E. H. Snow, H-P. Albus, A. Y. C. Yu,
D. A. Tremere

Fairchild Semiconductor
Division of Fairchild Camera and Instrument Corporation
464 Ellis Street
Mountain View, California 94040

Scientific Report No. 1

June 1969

Contract Monitor: Sven A. Roosild,
Solid State Sciences Laboratory

Prepared
for

AIR FORCE CAMBRIDGE RESEARCH LABORATORIES
OFFICE OF AEROSPACE RESEARCH
UNITED STATES AIR FORCE
BEDFORD, MASSACHUSETTS 01730

H7

AFCRL-69-0259

STUDY OF RADIATION EFFECTS ON
NOVEL SEMICONDUCTOR DEVICES

BY

E. H. Snow, H-P Albus, A. Y. C. Yu,
D. A. Tremere

Fairchild Semiconductor
Division of Fairchild Camera and Instrument Corporation
464 Ellis Street
Mountain View, California 94040

Prepared
for

ABSTRACT

A radiation resistant power JFET has been designed to have an I_{DSS}
of 4 amps, a pinch-off voltage of 8 volts and a breakdown voltage of
40 volts. The predicted change in I_{DSS} or G_m for this device after
10^{15} nvt is about 36%. Following this design, several runs of devices
have been fabricated and characterized. Outstanding problems include
high pinch-off voltages (probably due to the graded nature of the gate
junctions), low I_{DSS} (probably due to source and drain series resistance),
and low breakdown voltage (due to epitaxial defects in the large area
bottom gate). The best results to date are I_{DSS} = 2.5 amp with a
pinch-off voltage of 12 volts.

Several types of silicon planar Schottky barrier diodes have been
exposed to ionizing radiation and the same phenomena are observed
as on p-n junctions — increase in the fast surface state density and
the build-up of a positive space charge in the oxide. These cause
excess currents in the forward direction and "soft" reverse character-
istics. Aluminum diodes are relatively less affected by radiation
than platinum diodes because of the lower barrier height and higher
thermionic emission current of the former. The barrier height itself
does not change with radiation.

Capacitance-voltage and Hall effect measurements have been made on
high quality epitaxial GaAs before and after exposure to nuclear
reactor radiation. From changes in carrier concentration, a neutron
carrier removal rate of 6 to 8 cm^{-1} has been determined. From
changes in liquid nitrogen mobility (and some assumptions on scatter-
ing mechanisms), an introduction rate for ionized scattering centers
of 38±5 cm^{-1} has been determined.

TABLE OF CONTENTS

LIST OF ILLUSTRATIONS

LIST OF ILLUSTRATIONS
(Continued)

v

SECTION I

RADIATION RESISTANT POWER JFET

Introduction

The main goal for this portion of the contract is to apply the results
of the work reported under Contract AF19(628)-5747 to the design,
fabrication and testing of a practical radiation resistant power JFET.
Work accomplished in the first six months of this contract included
the design and fabrication of initial samples of that device.   This
section of the report is divided into the following areas:

- design
- fabrication details
- results obtained on initial devices
- discussion of results, problems and modifications.

Design

Under the previous contract, a JFET computer program and a graph
relating neutron radiation hardness to channel doping of a JFET were
developed and reported.   Both the program and the graph now have
been used to design a neutron radiation resistant power JFET.   Within
Fairchild Semiconductor, it was agreed upon developing a device with
a current capability of about 4 A, a reasonable radiation hardness at
doses up to 10^{15} nvt and a breakdown voltage comparable to bipolar
power devices.   As a result of the computer design work, Figure 1
shows a computer plot of the characteristics of a JFET with the
following specifications:

channel doping $N_D = 2 \times 10^{12} \, cm^{-3}$

channel length to width ratio $Z/L = 4500$

channel thickness $d = 1.5 \, \mu m$

1
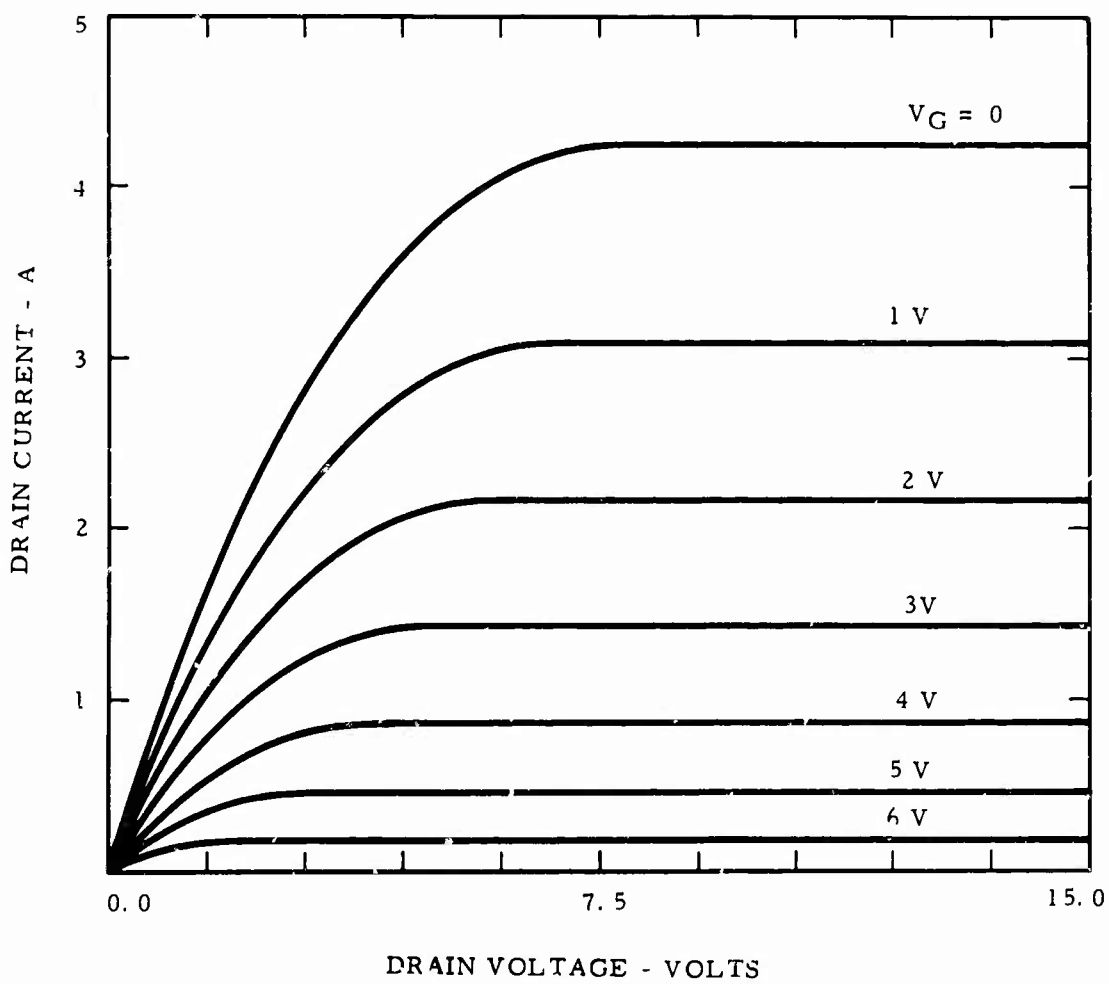
Figure 1. Predicted Initial I-V Characteristics for Power
JFET Design Discussed in the Text

2

The predicted maximum I_{DSS} is 4.24 A and the pinch-off voltage is about 8 V.* The maximum possible breakdown voltage for the 2×10^{16} cm^{-3} material will be 40 V.

Figure 2 shows a predicted plot for the same device after a fast neutron exposure of 10^{15} nvt. Carrier removal in the neutral channel as reported by Stein has been taken into account in the program and causes an I_{DSS} (or G_m) degradation of about 36%. The maximum I_{DSS} after 10^{16} nvt irradiation is 2.7 A.

According to these plots, the following specifications for a power junction FET for fast neutron environments have been proposed.

ELECTRICAL CHARACTERISTICS

Parameter	Conditions	Typical pre-irradiation value	Post 10^{15} nvt value
BV_{GSS}	$I_{GSS} = 10\ \mu A$	40 V	
I_{DSS}	$V_D = 10$ V, $V_G = 0$	4.25 A	2.75 A
V_T		8 V	
R_{on}	$I_D = 1.5$ A	1 Ω	1.6 Ω
G_m	$I_D = 1.5$ A	0.6 $\frac{1}{\Omega}$	0.5 $\frac{1}{\Omega}$
R_{TH}		3.5 °C/W	

Package: TO-59

The mask set for this power JFET has been designed:

The chip size is 85 $\times$ 110 mils,

the channel length is 0.3 mils, and

the channel width is 1300 mils. thus leading to a $Z/L = 4330$.

_____

*It was assumed that the gate junction is a perfect one-sided step junction. It is shown later that this is not relizable in practice.
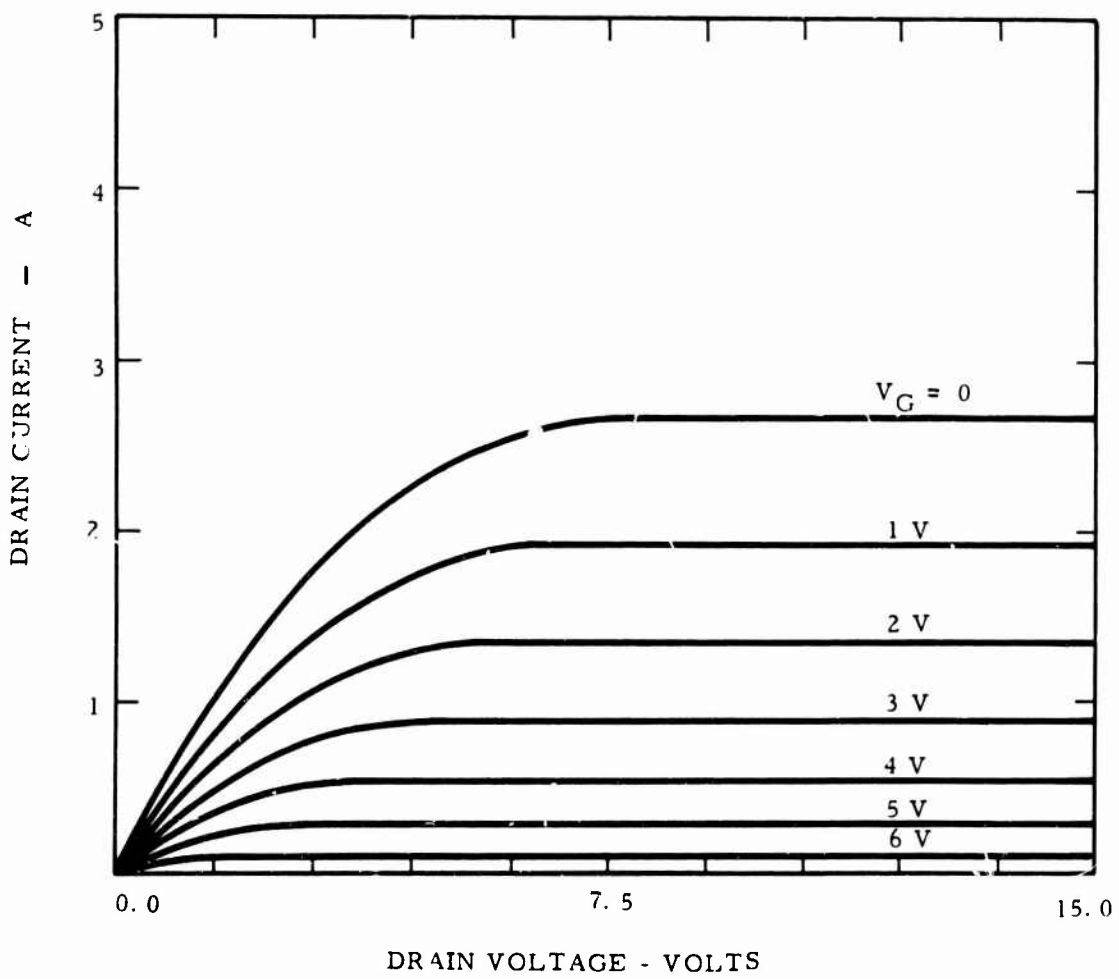
Figure 2. Predicted I -V Characteristics after 10^{15} nvt
Neutron Dose for Power JFET of Figure 1

4

Figure 3 shows the metal mask of that set and Figure 4 is a photo-
graph of a completed chip.

The metal pads are designed for one 14 mil and two 10 mil wires,
respectively. The Al layer thickness is to be 5 μm to ensure
adequately low current densities, source and drain fingers are 0.6 mil
wide, thus leading to a voltage drop along the longest finger (32 mils)
of about 50 mV and a maximum current density at the root of that
finger of 2.5 x 10^5 A/cm^2. The 0.7 mil metal stripe over the gate is
connected to the diffused gate at the bends in the "snake." The metal
extends 0.2 mil over the junction in order to optimize the breakdown
voltage.

Fabrication Details

Power JFETs have been built using the design parameters and a
processing scheme as shown in Table I. A cross-section of a typical
cell is shown in Figure 5. The oxide thickness has to be sufficient
for diffusion masking, but should be as thin as possible in order for
the field plates to be effective. [1] The oxide thickness chosen is
about 5000 Å. The requirements for the top gate diffusion and the
substrate doping are such that the depletion layer of both junctions
spread mainly into the channel when reverse biased. A high-frequency
transistor base diffusion, which approaches a step junction profile about
0.5 μm deep, is being used to form the top gate. For the bottom gate
junction, a compromise has to be made between a favorable high dopant
concentration ratio (C substrate to C channel) and the unfavorable
dopant redistributions caused by such a high ratio during epi growth
and isolation diffusion. To illustrate this, depletion spreading into a
2 x 10^{16} cm^{-3} doped channel for different substrate dopings and the
related outdiffusion have been calculated using Lawrence and Warner's[2]
curves. The results shown in Table II indicate that while in the case
of more graded junctions the ratio of depleting into the substrate is
higher, the total depletion width increases also, so that the amount of
depletion into the channel is about the same. Therefore, the lowest
substrate doping (2 x 10^{17} cm^{-3})should be used since it involves the
least amount of outdiffusion and provides comparable depletion width.

Another result of this comparison is that 12 V is a more realistic value
for the voltage necessary to pinch off a 1.5 μm wide channel than
8 V (spec.) as calculated on the computer assuming step junctions.
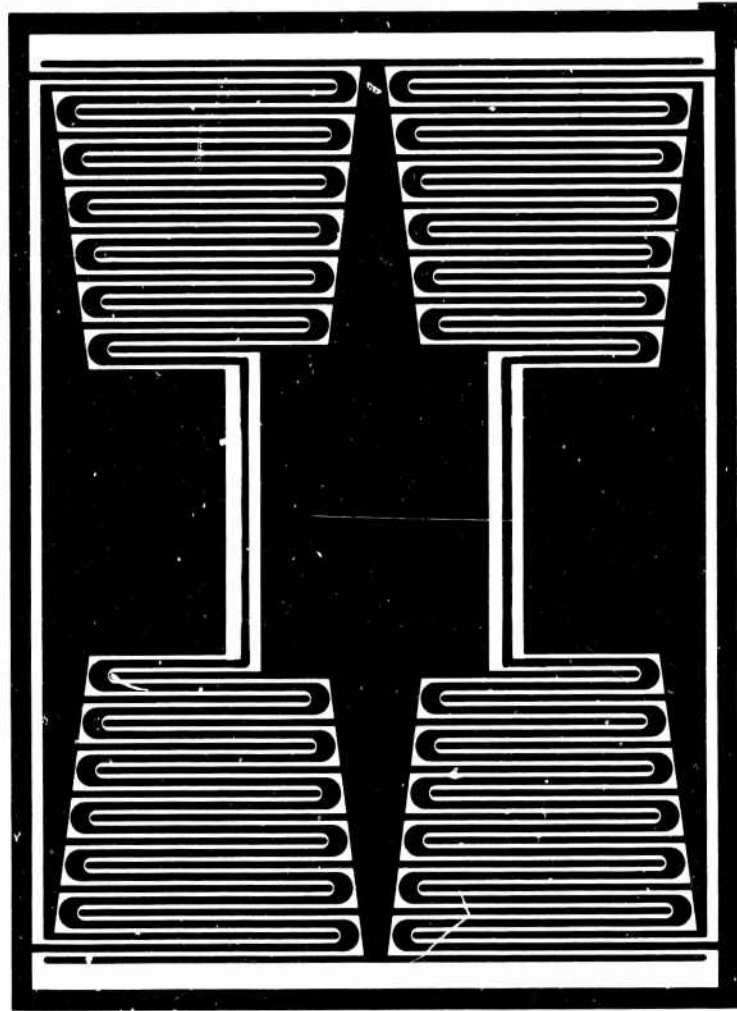
Figure 3.   Metal Mask of a Silicon Power JFET

6
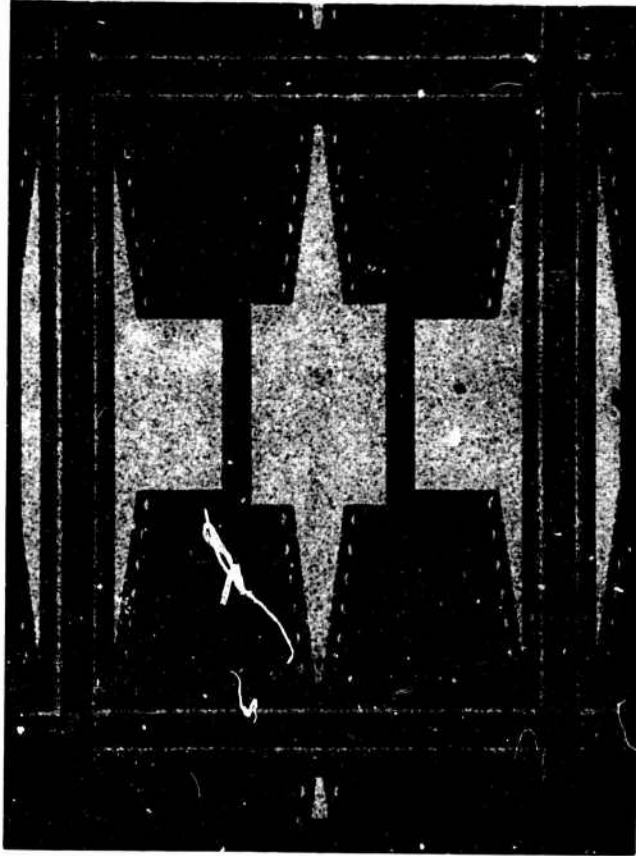
Figure 4.   Photograph of a Silicon Power JFET.

TABLE I

PROCESSING FLOW CHART FOR POWER JFET

p^+ substrate material

```
┌─────────────────────────┐          ┌─────────────────────────┐
│  n-epi deposition       │          │  source, drain contact  │
│                         │          │  n⁺-diffusion           │
└─────────────────────────┘          └─────────────────────────┘
            │                                    │
            ▼                                    ▼
┌─────────────────────────┐          ┌─────────────────────────┐
│  oxidation              │          │  gate contact oxide     │
└─────────────────────────┘          └─────────────────────────┘
            │                                    │
            ▼                                    ▼
┌─────────────────────────┐          ┌─────────────────────────┐
│  isolation oxide cut    │          │  metallization          │
└─────────────────────────┘          └─────────────────────────┘
            │                                    │
            ▼                                    ▼
┌─────────────────────────┐          ┌─────────────────────────┐
│  isolation predep +     │          │  metal pattern cut      │
│  diffusion              │          └─────────────────────────┘
└─────────────────────────┘                     │
            │                                    ▼
            ▼                         ┌─────────────────────────┐
┌─────────────────────────┐          │  metal alloy            │
│  gate oxide cut         │          └─────────────────────────┘
└─────────────────────────┘                     │
            │                                    ▼
            ▼                         ┌─────────────────────────┐
┌─────────────────────────┐          │  backlap and dice       │
│  gate diffusion +       │          └─────────────────────────┘
│  oxidation              │                     │
└─────────────────────────┘                     ▼
            │                         ┌─────────────────────────┐
            ▼                         │  assemble in TO59       │
┌─────────────────────────┐          │  package                │
│  source, drain contact  │          └─────────────────────────┘
│  oxide cut              │
└─────────────────────────┘
```
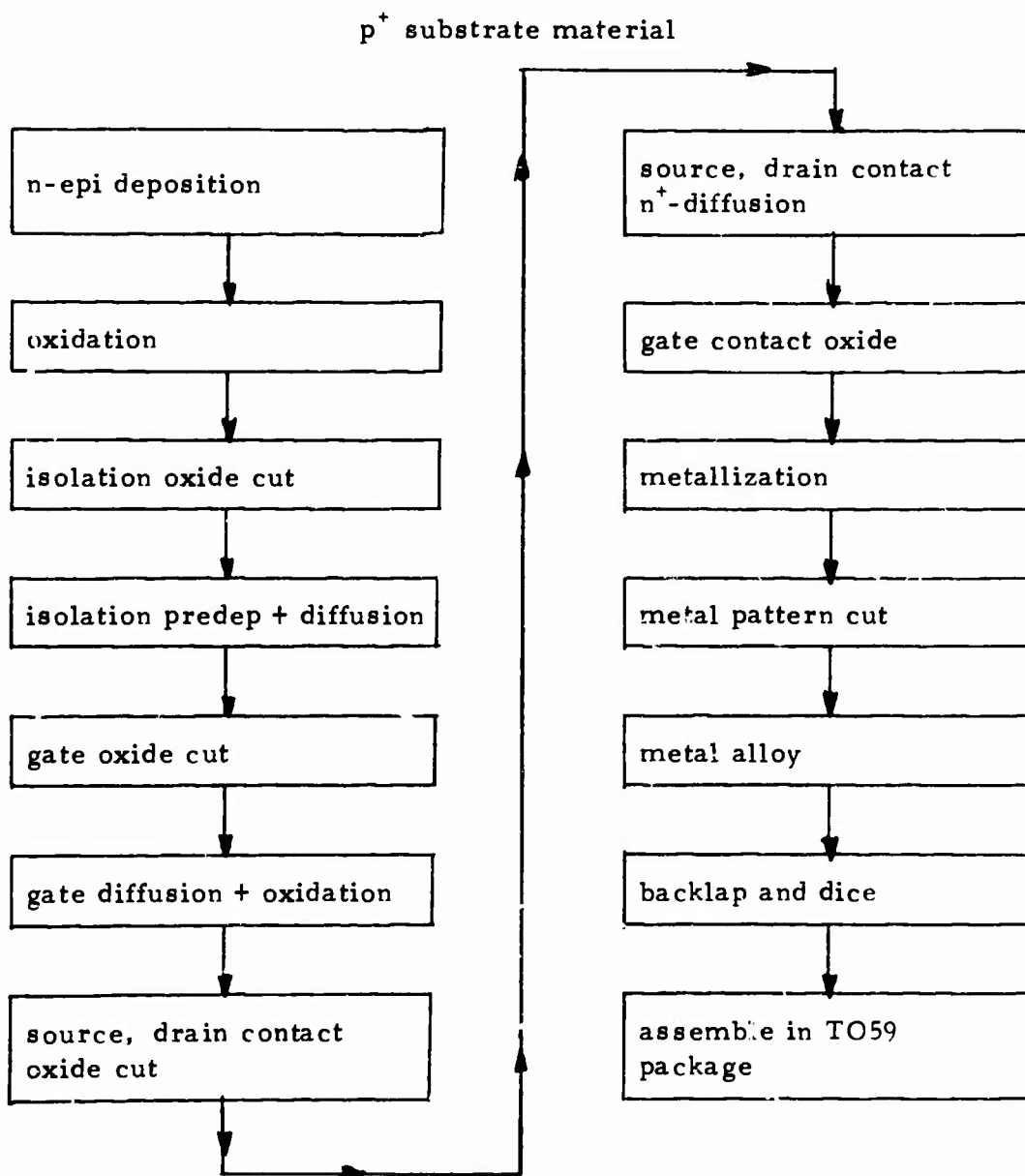
Figure 5.   Partial Cross Section of the Power FET

TABLE II

A: Depletion width into the channel for bottom gates corresponding
to various substrate doping concentrations. (Channel doping
concentration = 2 X 10^{16} cm^{-3}.)

Gate Voltage	Substrate Doping and Corresponding Outdiffusion Depth		
	2 X 10^{17}cm^{-3}, 0.5 μ	2 X 10^{18}cm^{-3}, 1.0 μ	2 X 10^{19}cm^{-3}, 2.0 μ
8 V	0.57 μ	0.55 μ	0.63 μ
12 V	0.72 μ	0.76 μ	0.77 μ

B: Depletion width into channel for top gates corresponding to
various assumed diffusion profiles (channel doping concentration =
2 X 10^{18}cm^{-3}, surface concentration = 2 X 10^{18}cm^{-3}, junction
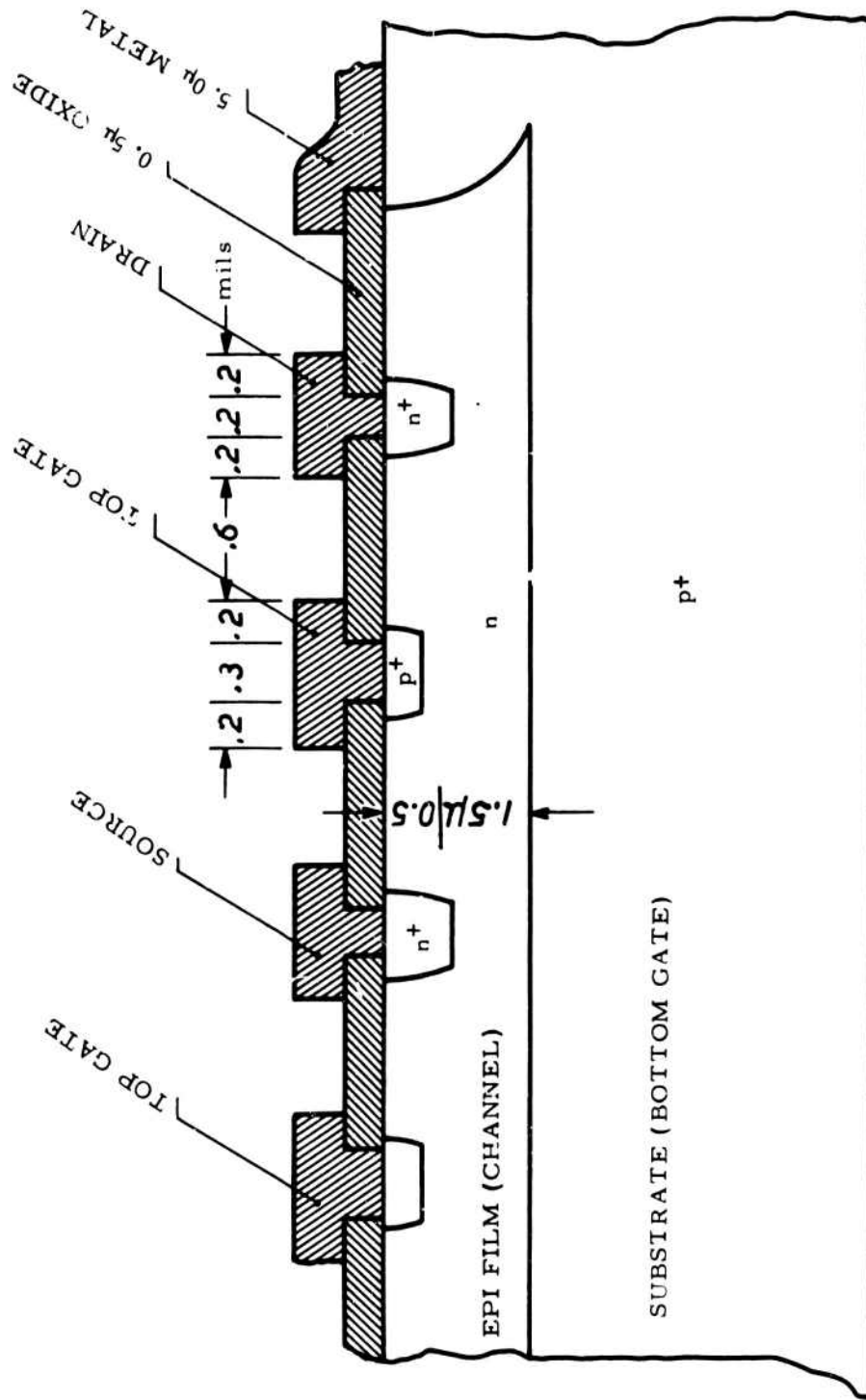depth = 0.5 μ).

Gate Voltage	Assumed Diffusion Profile		
	erfc	gaussian	box
8 V	0.62 μ	0.64 μ	0.70 μ
10 V	0.71 μ	0.73 μ	0.80 μ
12 V	0.77 μ	0.80 μ	0.90 μ

10

Results Obtained on Initial Devices

We have been able to build a few devices from runs with different substrate dopings and channel widths. The channel doping was between 1 and 2×10^{16} cm^{-3}. The maximum I_{DSS} achieved was 2.5 A. Figures 6 through 9 are curve tracer photographs of typical devices from various runs and Table III compares the results and run data.

Discussion of Results

The devices of run #4 cannot be pinched off completely due to a problem in the mask set which was corrected for the following runs. The breakdown voltage target of 40 V at 10 μA has not yet been achieved due to problems intoduced by random defects in the np$^+$ epi material. The breakdown voltage problems were related to the substrate-epi junction as follows. Epitaxially grown junctions are evaluated by using the power device isolation mask to etch mesa diodes (85 $\times$ 110 mils). The small JFET geometry (6.5 $\times$ 3) used for the work reported in the previous contract acts as a control. Initially, the yield for the large area was effectively zero, while the small area yield was approximately 80-90%. Even after a tremendous effort was made to avoid those defects during the deposition of the film, the yield of good devices is still small. A typical result is given below:

85 $\times$ 110 mils mesa	6.5 $\times$ 3 mils mesa
$\geq$ 40 V at 10 μA = 10%	= 82%
$\geq$ 40 V at 100 μA = 30%	= 90%

The actual breakdown voltage of this wafer is 50 volts.

Another reason for low breakdown voltages is because fieldplates used to minimize curvature effects of shallow diffused junctions are not very effective on these devices since it is difficult to deplete 2×10^{16} cm^{-3} n-type material. It is planned to grow a thin, more lightly doped, layer at the surface so that surface breakdown effects can be minimized. This will be done after we have a reasonably good control over the random defect problem.

Another serious problem is the discrepancy between the measured $I_{DSS} = f(V_T)$ and the theoretical expectations. The I_{DSS} for a given V_T is consistently lower than predicted. Comparing the 3 parts of run 12, one finds surprisingly an almost linear relationship between

11

Run - 4

Substrate Doping 10^{19} cm^{-3}, p

Channel Doping 1.9^{16} cm^{-3}, n

Top Gate 0.6 μm   Bottom Gate 1.8 μm
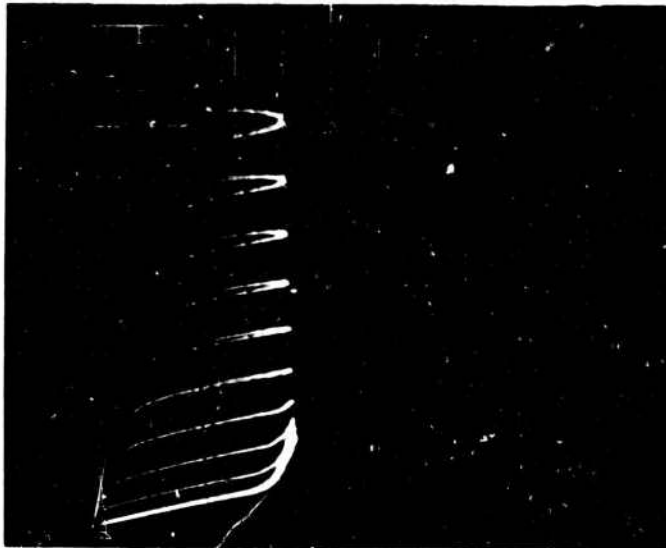
No. 3

I_{DS} = 200 mA/div

V_{DS} = 5 V/div

V_G = -1 V/step

No. 5

Figure 6.   I-V Characteristics of Typical Devices from Run 4

Run-10

Substrate Doping 6×10^{18} cm^{-3}, p

Channel Doping 1.4×10^{16} cm^{-3}, n

Top Gate   0.5 μm   Bottom Gate 1.8 μm

No. 52

I_{DS} = 200 mA/div

V_{DS} = 2 V/div

V_G = -1 V/step
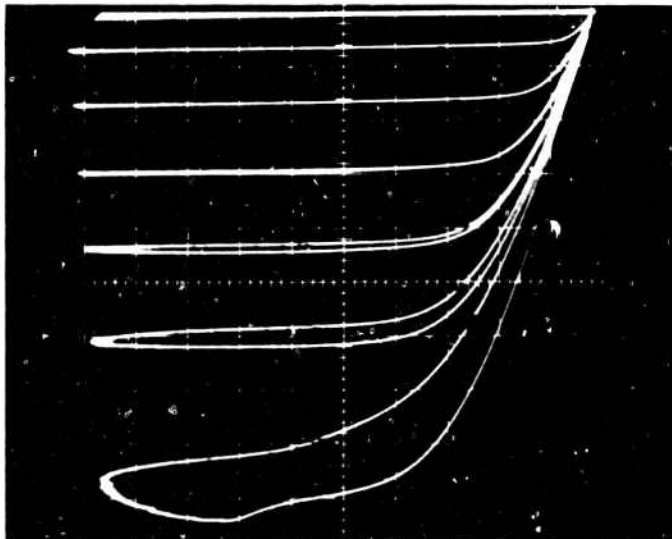
No. 56

Figure 7.   I-V Characteristics of Typical Devices from Run 10

13

TABLE III

RESULTS OF VARIOUS JFET RUNS

Run No.	Substrate doping	Channel doping	Channel width	Top gate depth	I_{DSS} $V_G=0$	V_T	G_m $V_G=0$	BV$_{GSS}$ 100 µA	BV$_{GSS}$ 2 mA
4	10^{19} cm^{-3}	1.9×10^{18} cm^{-3}	1.2 µm	0.6 µm	1.6 A	9 V	0.240 $\frac{1}{\Omega}$	~25 V	~30 V
10	6×10^{18} cm^{-3}	1.4×10^{18} cm^{-3}	1.3 µm	0.5 µm	1.0 A	6 - 7 V	0.230 $\frac{1}{\Omega}$	~33 V	~40 V
12A	5×10^{17} cm^{-3}	1.1×10^{16} cm^{-3}	1.35 µ	1.5 µm	1.1 A	6 - 7 V	0.240 $\frac{1}{\Omega}$	~32 V	~40 V
12B	5×10^{17} cm^{-3}	1.1×10^{16} cm^{-3}	1.8 µ	1.2 µm	2.4 A	12-14 V	0.500 $\frac{1}{\Omega}$	~20 V	~35 V
12C	5×10^{17} cm^{-3}	1.1×10^{16} cm^{-3}	0.75 µ	1.7 µm	0.25 A	2 V	0.035 $\frac{1}{\Omega}$	~20 V	~35 V

Run - 12A

Substrate Doping	5×10^{17} cm^{-3}, p
Channel Doping	1.3×10^{16} cm^{-3}, n
Top Gate 1.5 μm	Bottom Gate 2.85 μm
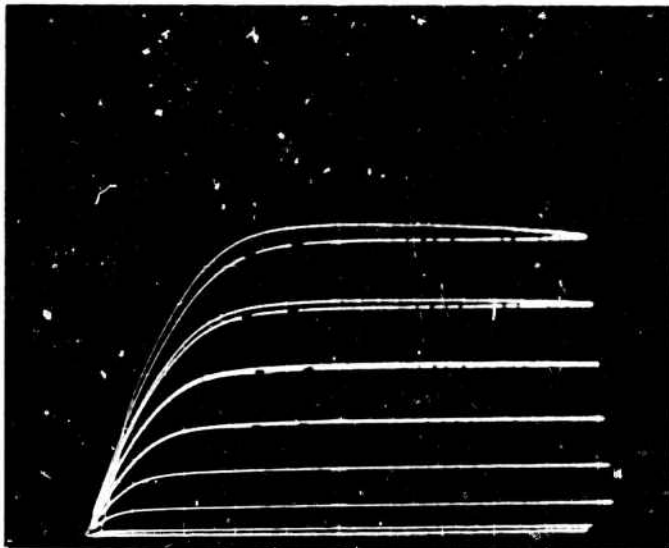
No. 17

I_{DS} = 200 mA/div
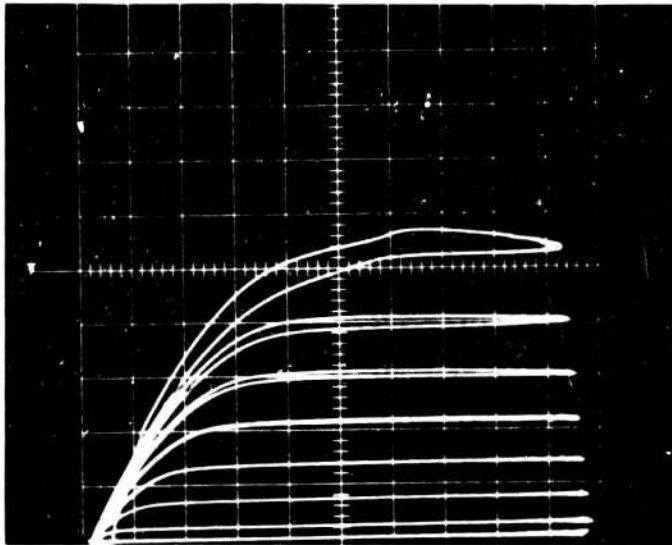
V_{DS} = 2 V/div

V_G = .1 V/step

No. 18

Figure 8.   I-V Characteristics of Typical Devices from Run 12A

Run - 12C

Substrate Doping $5 \times 10^{17} \text{cm}^{-3}$, p

Channel Doping $1.3 \times 10^{16} \text{cm}^{-3}$, n

Top Gate 1.2 μm   Bottom Gate 3.0 μm

No. 6

I_{DS} = 400 mA/div

V_{DS} = 2 V/div

V_G = -2 V/step

No. 10

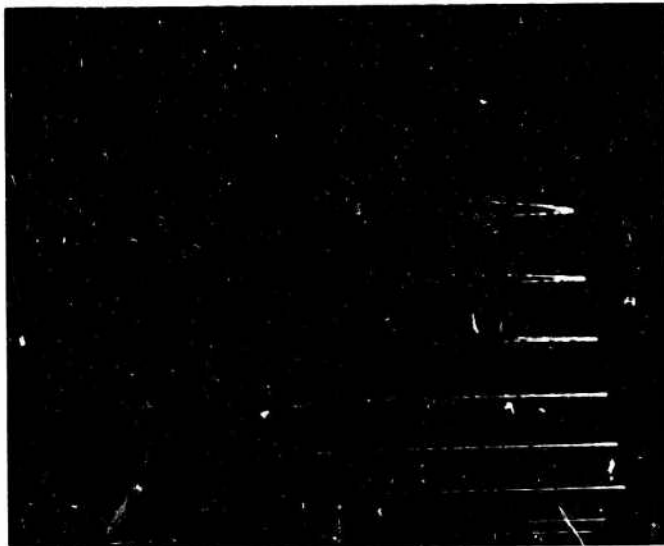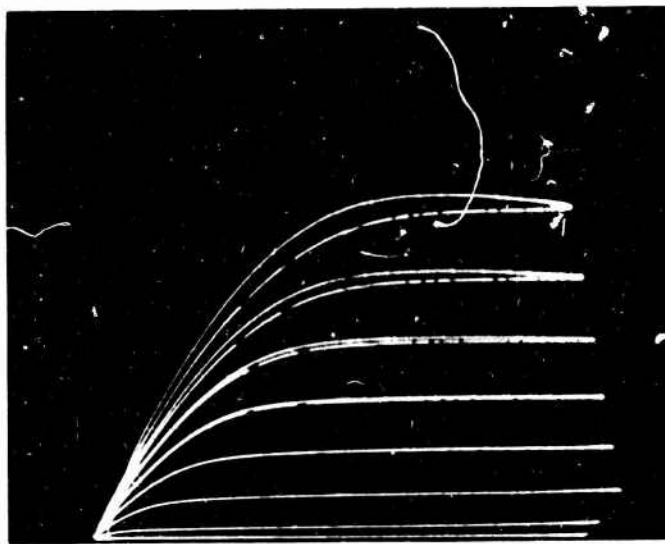Figure 9.   I-V Characteristics of Typical Devices from Run 12C

16

I_{DSS} and V_T for three different channel widths (Figure 10) which were obtained by different diffusion depths. According to Cobbold[3] one would expect $I_{DSS} \sim V_T^{3/2}$ for an epi-JFET with abrupt gate junctions or $I_{DSS} \sim V_T^{5/3}$ for a double diffused JFET.

The non-agreement is probably due to the fact that we neglected the depletion at zero bias and the series resistance. For devices with a narrow channel the zero bias built in voltage has to be taken into account. So the total voltage causing the pinch off of devices of run 12B is probably close to 3 V. On the other hand, at high current densities series resistances cannot be neglected. R_S and R_D are estimated to be about 2.5 times the resistance of the metallurgical channel since the n^+ diffused source and drain areas are 1 mil away from the 0.3 mil wide channel and the channel width is only about 25% narrower than the film.

This large distance is required for definition of the thick (5 μ) double ring field plate structure (see Figure 5). The results of runs 4 and 10 fit into the same plot in Figure 10 even though they are fabricated using different material and processing. This implies that a design parameter like the series resistance controlled by the mask is responsible for the consistent results. We are trying to demonstrate this with an optional mask for the n^+ contact diffusion which allows us to reduce R_S and R_D by a factor of 3.

Conclusions

A JFET computer program and a graph relating neutron radiation hardness to channel doping of a JFET developed under the previous contract were used to design a 4 A/40 V device for doses up to 10^{15} nvt. Various devices with channel dopings between 1 and 2×10^{16} cm^{-3} were fabricated and the results reported. The maximum current-capability achieved so far is 2.5 A with a 14 V pinch off voltage. We have encountered two major problems. First the breakdown voltage is limited mainly by serious defect problems in the epi-grown junction to values between 20 and 35 V. Second, the application of these devices is limited by the low I_{DSS}/V_T ratio which is believed to be due to series resistance problems. Our future work will concentrate on these two problems. Increasing the Z/L ratio to increase the I_{DSS}/V_T ratio does not seem to be feasible because of the yield problems already apparent.

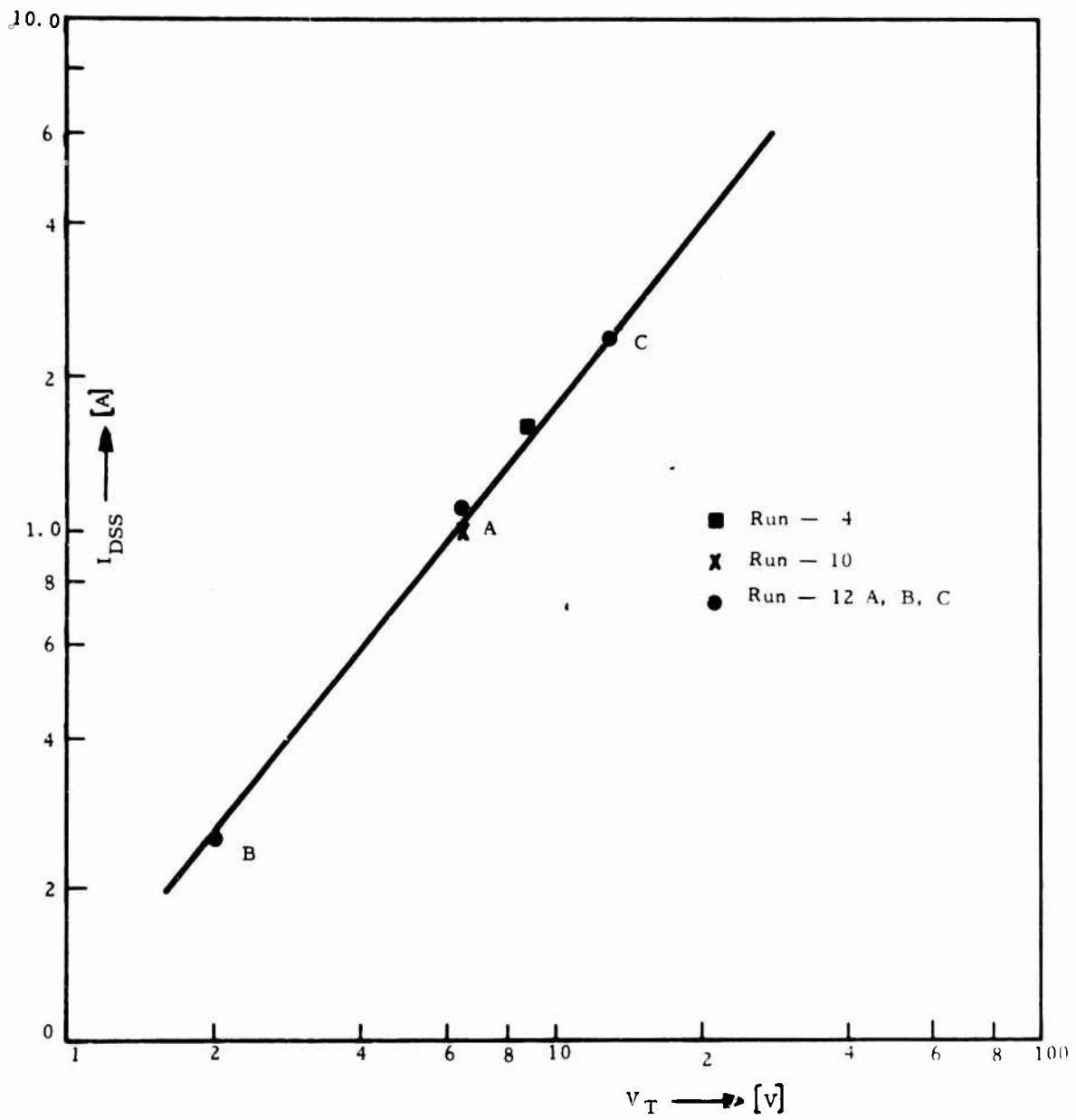The devices reported will be used for neutron radiation experiments.

Figure 10. I_{DSS} ($V_G = 0$) vs Pinch-Off Voltage of Devices from various Runs

18

SECTION II

RADIATION EFFECTS ON SILICON SCHOTTKY BARRIERS

Introduction

Since recent research and development efforts at various laboratories have produced Schottky barriers on Si with near-ideal characteristics,[4-7] there has been a renewed interest in these devices. Schottky barriers are ideal for microwave and switching applications because of their lack of minority carrier injection.[8] In addition, important new applications are: Schottky barrier "clamps" on the collector-base junction of transistors to improve switching performance;[9] Schottky barrier gates on field-effect transistors operative in the microwave region[10-12] and various gating, and clamping applications.[13] Radiation effects on a number of Si Schottky barriers have been examined in the past.[14,15] However, in view of the increasing importance of Schottky barriers, a comprehensive study of the radiation effects on these devices is desirable. In this work, a variety of Schottky diode structures were used, including the guard ring structure. In addition, gate-controlled Schottky diodes[8] were employed to unambiguously separate surface from bulk effects. The following areas are disucssed in this section:

- radiation effects on Silicon Planar[®] p-n junction devices
- effects of ionizing radiation on Si-Schottky barriers
- nuclear radiation effects on Schottky barriers

Radiation Effects on Si-Planar[®] p-n Junctions

The two main permanent effects of ionizing radiations (e. g., low energy electrons, X-rays and γ-rays) on Si planar p-n junctions are: buildup of a positive space charge in the oxide and increase of surface recombination velocity (s_o).[16] They are both surface effects. These

_____

[®]Planar is a Fairchild patented process.

19

phenomena lead to reverse current degradation and excess current in the forward direction . Nuclear reactor radiation consists of both ionizing and neutron radiations. The main effects of neutron irradiations are: carrier removal and decrease in lifetime,[17] both bulk effects. These phenomena lead to excess forward and reverse currents and increase in series resistance of p-n junctions.

It is expected that all these effects should be present in Si Schottky barriers. However, since the thermionic emission current in Schottky barriers is much larger than diffusion currents in p-n junctions, it is also expected that radiation effects will not change the I-V characteristics of Schottky barriers as drastically as they do p-n junctions.

Effects on Ionizing Radiation on Si-Schottky Barriers

Experimental Methods

Four different structures of Schottky barrier diodes were used (Figure 11). Figure 11(a) shows a gate-controlled Schottky barrier diode in which the surface potential can be independently varied by applying a voltage to the gate electrode (G). An overlap structure (Figure 11(b)) has metal overlap over the oxide to act as a field plate. This is used to keep the underlying surface in depletion when the diode is reverse biased to avoid excess current at the corner. Figure 11(c) shows a structure with no metal overlap. In general, this structure has nonreproducible characteristics and poor radiation tolerance. The last structure (Figure 11(d)) has a p-n junction guard ring around the periphery of the Schottky barrier.[4,5] Three Si dopings were used: 6×10^{13}, 2.5×10^{15} and $1.2 \times 10^{16} cm^{-3}$. Both Al and Pt were evaporated on Si by electron-beam gun to form Schottky barriers. In the case of Pt Schottky barriers,the Si wafer was heated to 400°C during metal deposition, thus forming a platinum silicide. Regular photoresist techniques and lifting (for Pt) were used to define device geometry. More discussion of the fabrication method has been published elsewhere.[6,7]

Ionizing radiation was provided by low energy (15-20 keV) electron bombardment. The determination of dosimetry has been discussed previously.[18] Since the radiation effect has been shown to be independent of dose rate, only the total dosage is recorded. Typically the dose rate used was about 10^5 rad/sec. I-V and C-V (100 kHz) characteristics were measured by conventional methods.
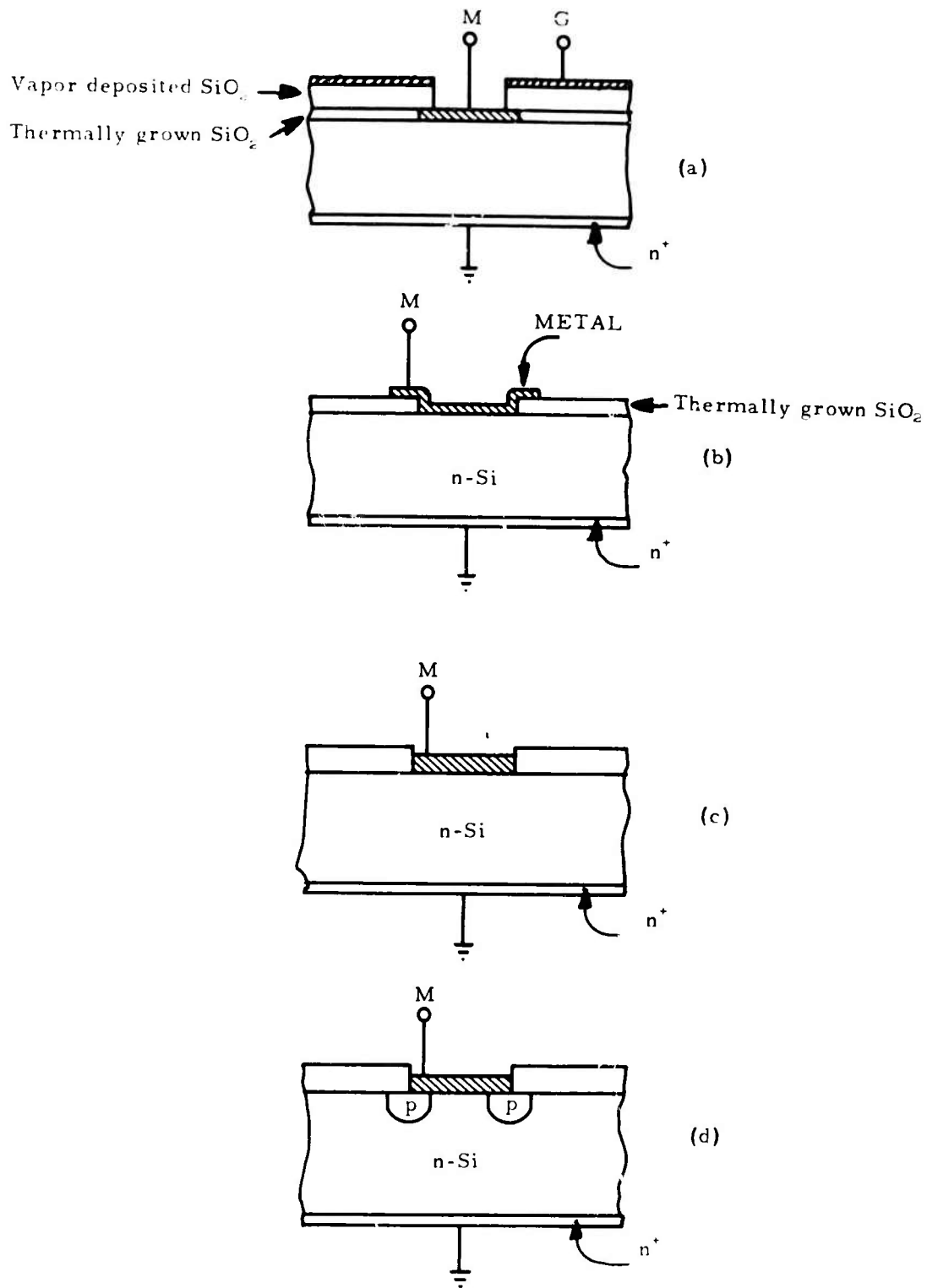
20

Figure 11.   Structure of various Schottky Barrier Diodes:
(a) gate controlled diode; (b) overlap diode;
(b) no overlap diode; (d) p-n guard ring diode

21

Experimental Results

In Figure 12 the capacitance of the gate (C_G) of a typical gate controlled
Pt Schottky diode, normalized to the capacitance of the oxide (C_o)
after various doses of electron radiation is plotted as a function of
the gate voltage V_G with a fixed reverse bias of 10 V on the Pt
electrode. Two effects are immediately clear: the flatband voltage
is shifted to more negative values and the C-V curve has considerable
broadening after radiation. The first effect is due to positive space
charge in the oxide[16] and the second one is due to increase of surface
state density.[16] Similar behavior is seen on gate-controlled Al-
Schottky diodes. Figure 13 shows the forward characteristic of the
gate-controlled Pt-Schottky diode after various doses of radiation.
The insert shows the gate voltage dependence of the forward current
at 0.1 V bias voltage. The curve before radiation is similar to that
reported before.[8] The increase in the current as the surface is
accumulated $(V_G \gtrsim + 20 \text{ V})$ is due to excess current around the
corner of the contact. The step increase in the current as V_G is
made more negative than -15 V is due to recombination in the field-
induced-junction formed beneath the gate. From the size of this
step, minority carrier lifetime is found to be 10^{-5} sec, in agreement
with earlier measurement.[8] After 10^8 rad radiation, the flatband
voltage is seen to be shifted to the left, due to positive space charge
in the oxide and a surface recombination peak appears at $V_G \approx -30$ V.
The surface recombination velocity (s_o) is found to be 130 cm/sec,
in fair agreement with earlier study on p-n junctions.[16] As the
electron dosage is increased, the flatband point is shifted further
to the left. At 10^8 rad, the flatband voltage is so large that even
at zero gate voltage, large excess current is flowing. This is
evident if one examines the I_F vs V_F plot with $V_G = 0$. Before
radiation, the forward characteristic is linear over about three
decades. After 10^8 rad, large excess current appears at low
forward bias due to strong accumulation of the surface which is
caused by positive space charge in the oxide.

Since the barrier height of Al Schottky barriers is only 0.69 eV[7]
compared with 0.85 eV[4] for Pt Schottky barriers, the current in
the former is more than two orders of magnitude higher. Therefore,
the excess current after radiation is completely masked for Al
Schottky barriers, and the forward characteristic is insensitive to
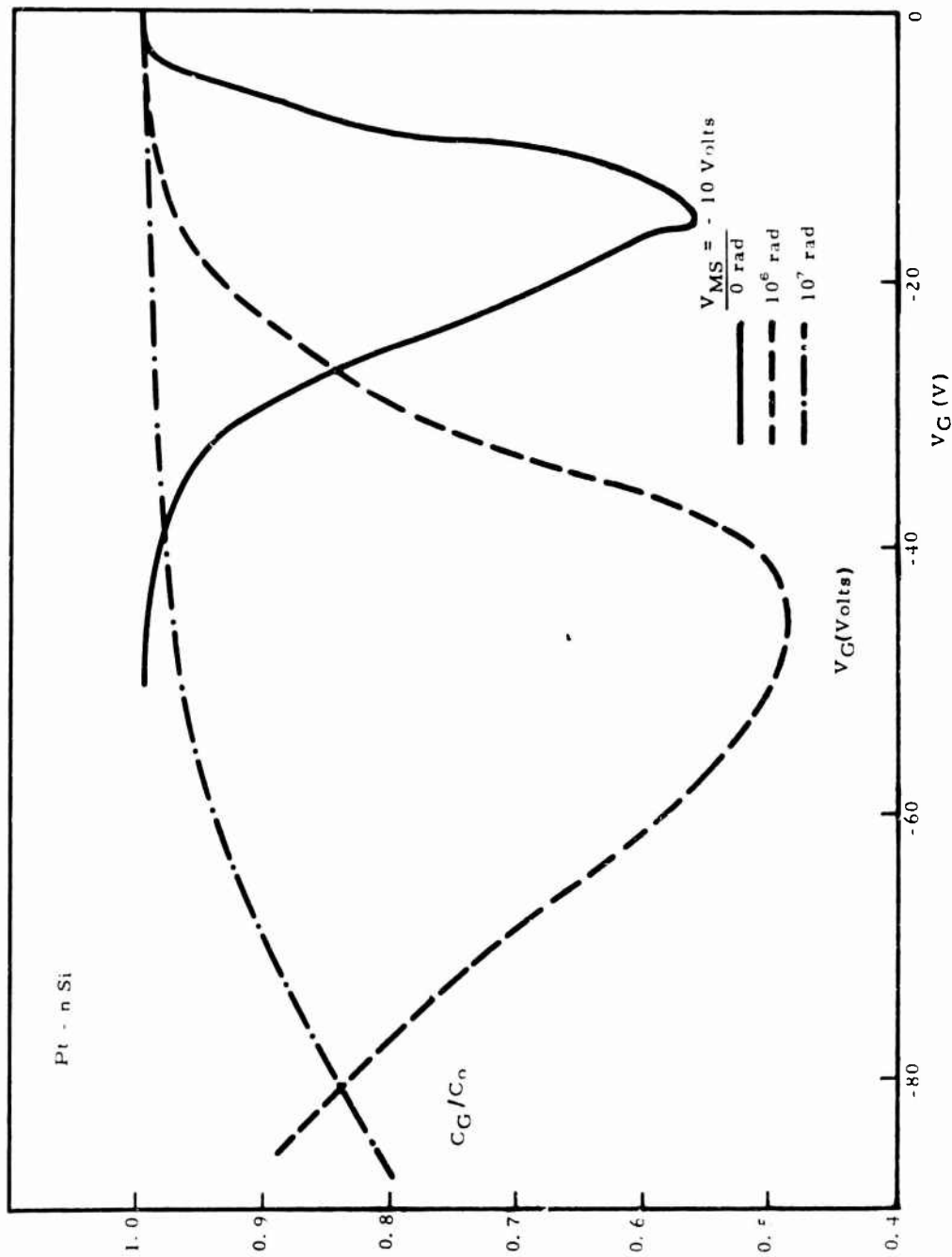electron radiation up to 10^8 rad.

Figure 12. Capacitance of the Gate (C_G) Normalized to the Capacitance of Oxide (C_O) as a Function of Gate Voltage (V_G) after various Electron Radiation Doses for Gate-Controlled Pt Schottky Diode
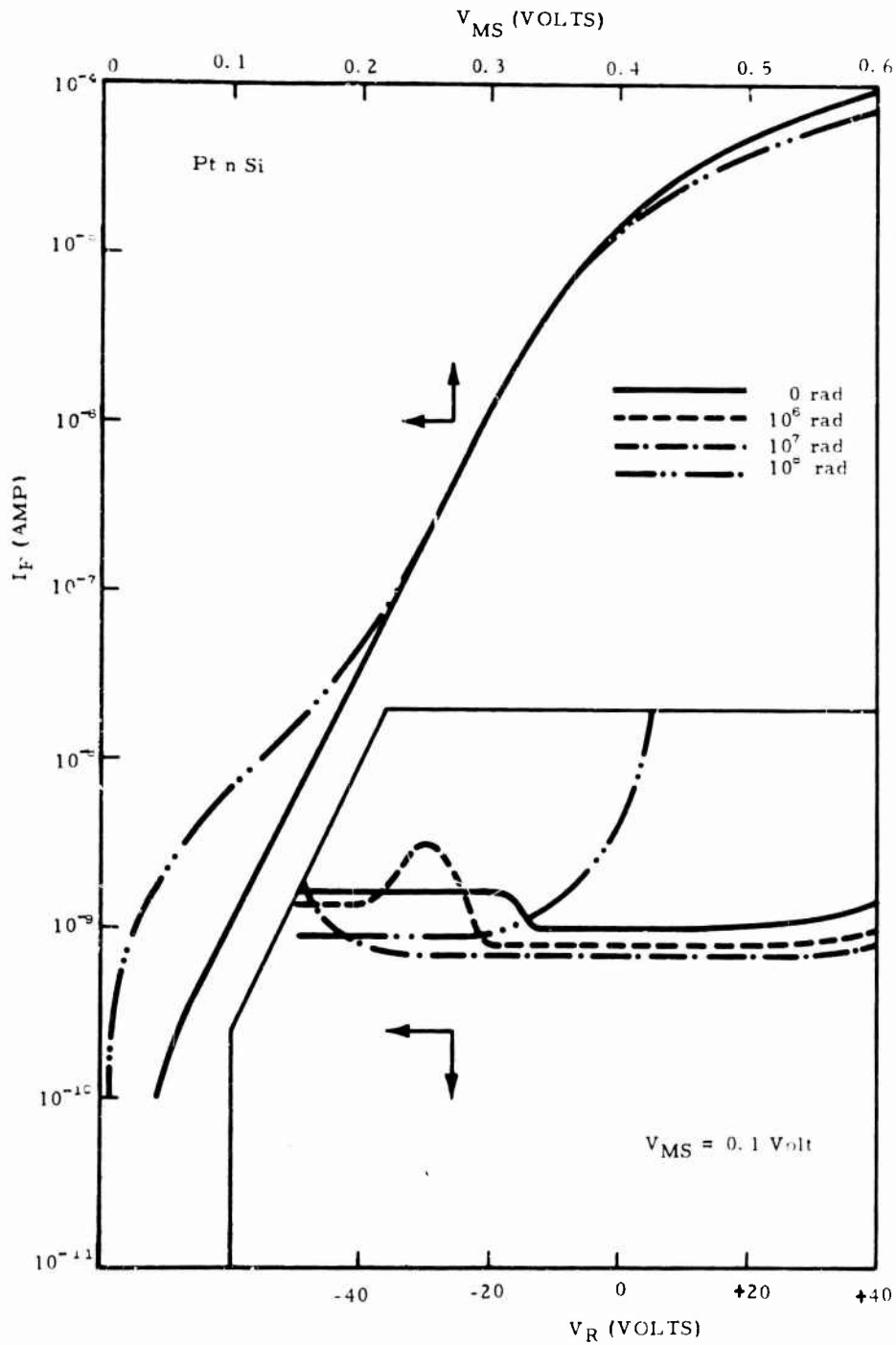
23

Figure 13. Forward I-V Characteristic of Gate-Controlled Pt
Schottky Diode. (Insert shows the gate voltage
dependence of forward current)

24

Figure 14 shows the reverse characteristic of the gate-controlled Pt-Schottky barrier. The flatband voltage is again seen to be shifted to more negative values and the s_o peak appears after radiation, consistent with the forward characteristic. The reverse current increases manyfold due to excess current around the corner. Similar behavior is observed on gate-controlled Al-Schottky barriers, although the percentage of reverse current increase is much less since the barrier height of Al Schottky diodes is lower.

The flatband value of the forward and reverse current is fairly insensitive to radiation up to 10^8 rad, indicating that the barrier height is little affected by electron irradiation. Annealing at 220°C for 1 1/2 hours after 10^9 rad is able to recover the characteristic to its initial form.

From Figures 13 and 14, it is clear that the degradation of the I-V characteristic after ionizing radiation is entirely due to oxide positive space charge which strongly accumulates the surface. It is a surface effect. Since the excess current is due to oxide positive space charge right next to the metal-semiconductor contact, it appears that the guard-ring structure should be ideal in eliminating this effect. Al Schottky barriers with structures shown in Figure 11(b)-(d) have been subjected to electron radiation. Structure (c) is very sensitive to radiation since there is no metal overlap to compensate the positive space charge in the oxide under reverse bias. Comparison of reverse current at 10 volts bias with or without guard ring is shown in Figure 15. The reverse current of the guard ring structure is unaffected until 10^9 rad, while that of the overlap structure increases manyfold after radiation.

Summary

From examining the gate-controlled Pt Schottky diode characteristics, it is concluded that the effects of ionizing radiation are due to positive space charge in the oxide. The Al-Schottky barrier is less sensitive to radiation since its barrier height is lower than that of Pt Schottky diode. Among the structures studied, guard-ringed Al-Schottky barrier diodes are the most radiation resistant and are immune to ionizing radiation up to 10^8 rad. The guard ring separates the oxide space charge from the corner of the metal-semiconductor contact, thus eliminating excess current at the corner region. However, for very high dosage ($\gtrsim 10^9$ rad), the guard-ring itself will eventually be degraded due to formation of field-induced junction at the surface.[19]
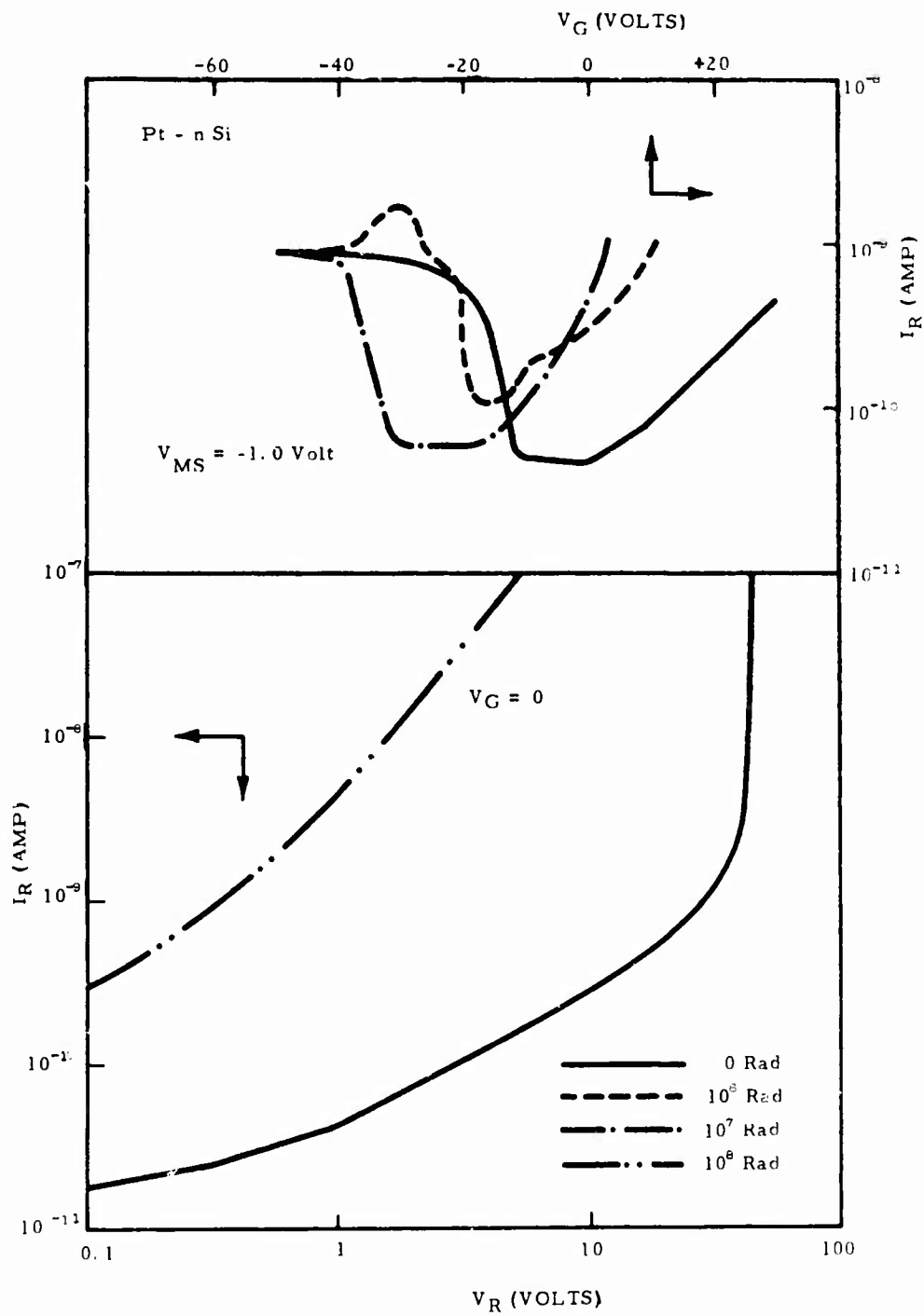
Figure 14. Reverse I-V Characteristic of Gate-Controlled Pt
Schottky Diode. (Insert shows the gate voltage
dependence of reverse current)

26
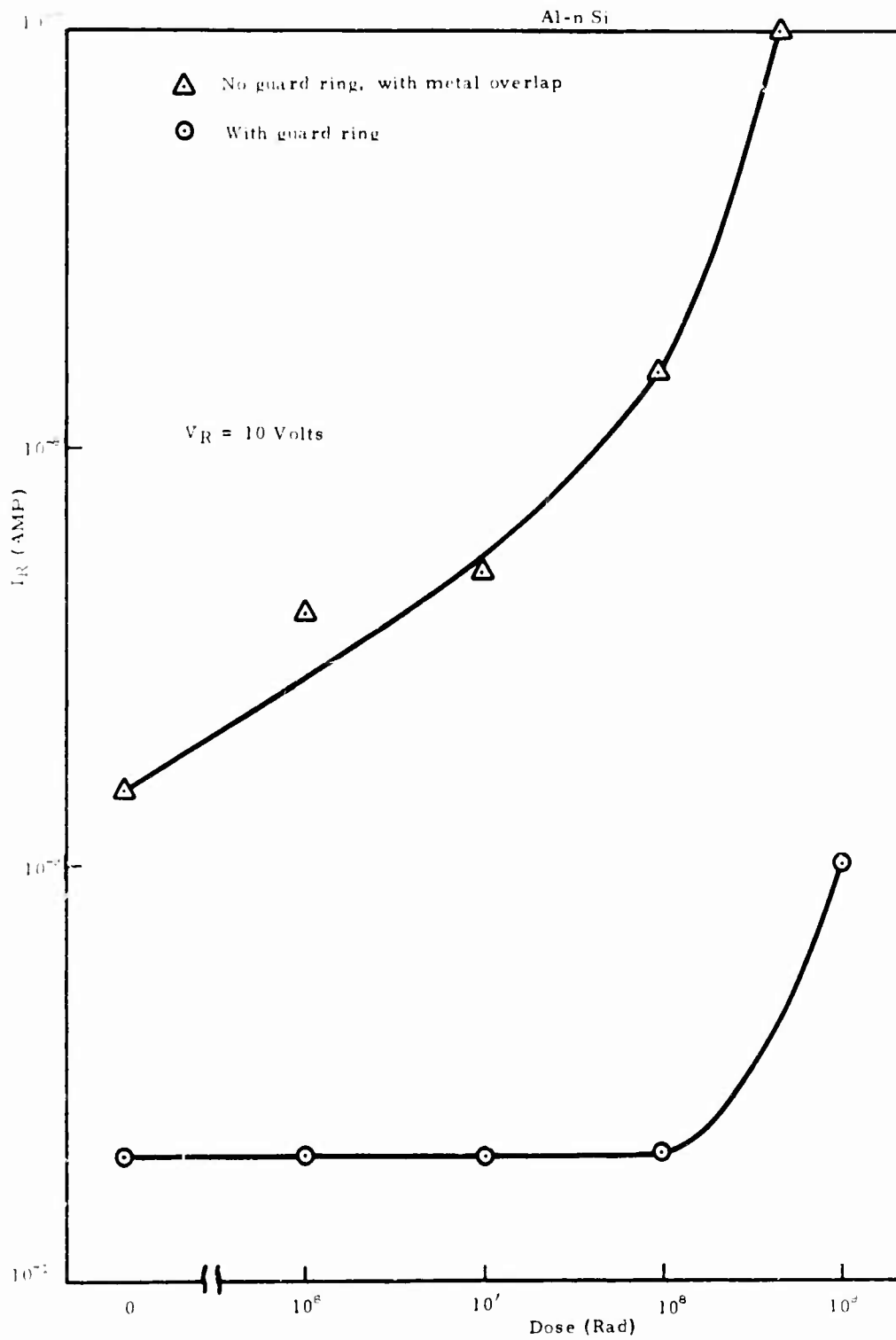
Figure 15.   Comparison of I_R at $V_R = 10$ volts for Al Schottky
Barrier with and without Guard Ring after various
Electron Radiation Dosages ($N_D = 1.2 \times 10^{16} cm^{-3}$)

27

Nuclear Radiation Effects on Schottky Barriers

Experimental Methods

Schottky barriers similar to those discussed in the last section were used
for nuclear radiation studies. The nuclear radiations were done
at Sandia Laboratory. Fast neutron doses (0. 1 to 6 MeV) of
10^{14}, 3×10^{14} and 10^{15} nvt were employed.

Experimental Results

Experimental data are currently being taken and analyzed. However,
one feature of nuclear radiation can be discussed at the present time.
From the series resistance of the Schottky diodes and their geometry
the resistivity of Si can be calculated. Thus, this can be used to
examine the effect of carrier removal due to neutron radiation.
The result of this study is shown in Figure 16. The points are
experimental data and the lines are theoretical calculations using
the following empirical relationship. [20]

$$n \; (\varphi) = n(o) \exp \left(- \; \varphi/k \right)$$

where

$$K = 600 \quad n(o)^{\,0.77}$$

the agreement is very good indeed. A complete discussion of effects
of nuclear radiation will be included in the next scientific report.
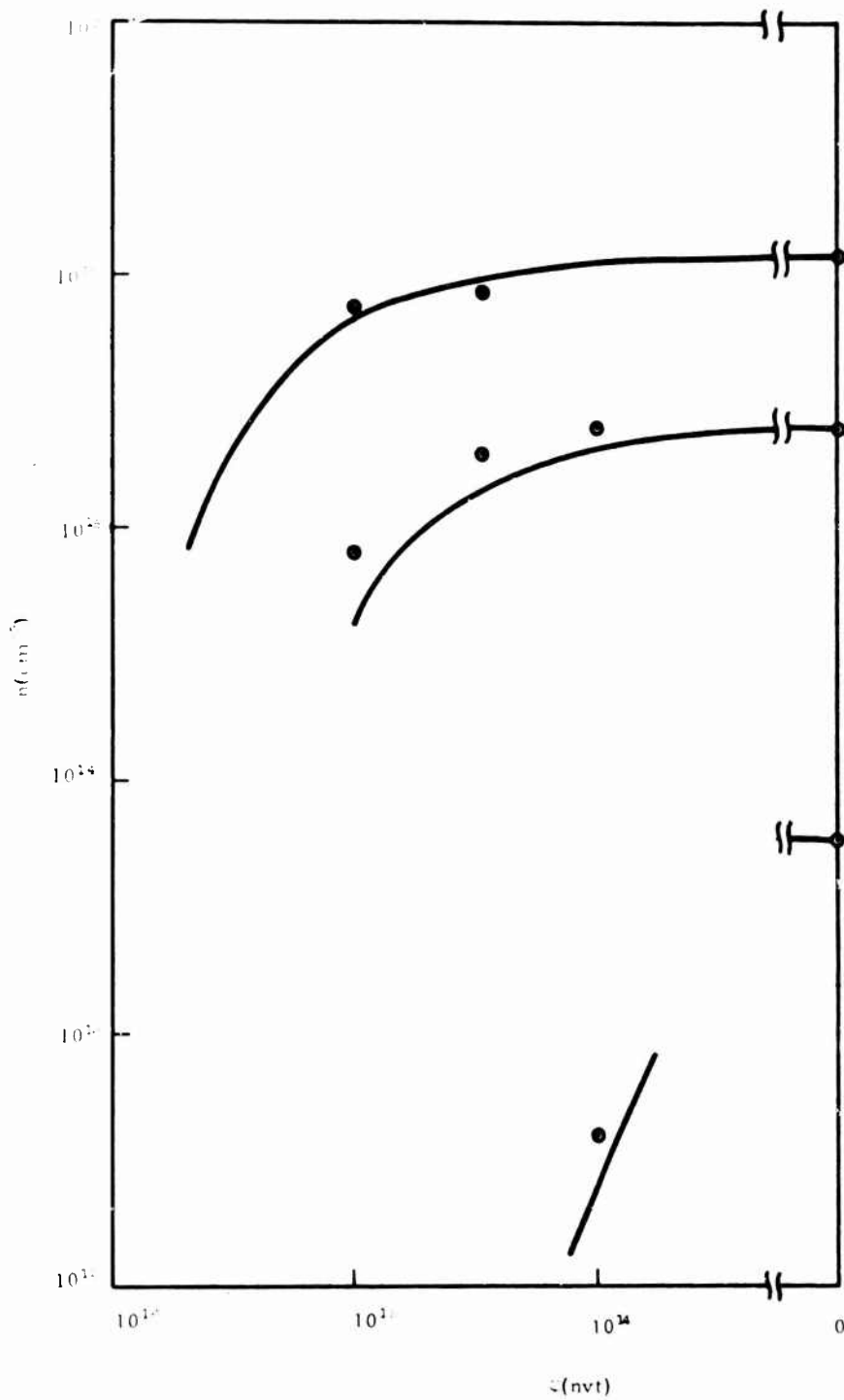
Figure 16. Plot of Carrier Concentration (n) versus Nuclear
Radiation dose φ. (The lines are theoretical and
the points are experimental)

29

SECTION III

NEUTRON RADIATION EFFECTS ON GALLIUM ARSENIDE

Introduction

The main objective of this work is to evaluate the effects of high
energy neutron irradiation on high quality, epitaxial gallium arsenide
films. The investigation is proceeding in three stages:

- a preliminary experiment, in which three groups of
  samples each group covering a wide range of doping,
  were exposed to three different neutron dosages to
  get a rough measure of the magnitude of the carrier
  removal effect,

- a detailed material study in which high quality films are
  given successive neutron dosages so that, hopefully,
  a more detailed description of the resultant compensation
  effect can be given,

- a device study in which various available devices
  which have been fabricated in epitaxial material such
  as Schottky barrier diodes, field effect transistors and
  p-n junction diodes will be irradiated and the results
  correlated with the results of the material investigation.

The preliminary experiment is complete and was discussed in the
first quarterly report. The work is currently concerned with the
detailed material study.

Sample Description

The sample for the material study is a clover leaf (van der Pauw)[21] Hall effect geometry ultrasonically cut through the backside to the front of the wafer. The specimen is thoroughly cleaned and given a light etch before demounting, i. e., while the front side with the epitaxial film is still protected. After demounting, the sample is again thoroughly cleaned in non-etching solvents. Small tin contacts are alloyed on the outer edge at the center of each leaf.

The material consists of an n-type, epitaxial film a few microns thick grown on a semi-insulating, chromium compensated, (100) oriented substrate. The films are grown by vapor phase transport[22] using high purity G_a, $AsCl_3$ and H_2. Typical impurity profiles of this material as obtained by differential capacitance[22] show the doping to be nearly constant near the surface and then decrease very quickly to an insignificant level ($\leq 10^{12} cm^{-3}$) at some point within the epitaxial film. The thickness at which the doping decreases abruptly is generally less than the total film thickness, possibly due to the presence of a substrate depletion layer. Nevertheless, the point where this occurs serves to define an effective film thickness. In addition to the above complication, evidence indicates that gallium arsenide has a surface space charge layer due to a high density of surface states which pin the Fermi level at the surface at a point approximately one-third of the energy gap up from the valence band.[23] A typical doping profile is shown in Figure 17.

Experimental Techniques

The usual procedure to evaluate the sample either before or after irradiation is to measure the Hall effect[21] at room and liquid nitrogen temperatures. From these measurements the mobility and the Q are calculated. The Q is defined as

$$Q_H = \int_{W_o}^{\infty} N(x) \, dx$$

where $N(x)$ is the doping at a point x into the film. The integral limits are from W_o, the boundary of the surface space charge, to

31

any large distance since the doping suddenly decreases to effectively zero after the effective film thickness is reached. It has sometimes been the practice to calculate a Hall doping concentration by dividing Q_H by the total film thickness--this number never agrees with the Schottky barrier results on these films because of the surface depletion layer and because the total film thickness is always greater than the effective thickness.

Next aluminum Schottky barrier diodes approximately 10 mils in diameter are evaporated through a metal mask on to the center of the van der Pauw sample. The mask is so arranged that the aluminum covers most of the material outside of the center including the contacts to reduce the series resistance. A capacitance--reverse bias voltage curve is plotted where, if the film is thin enough, the capacitance suddenly decreases to nearly zero at a point corresponding to the effective film thickness. The voltage at this point is designated V_P, the pinch-off voltage. From this curve is calculated

$$Q_{SB} = \frac{1}{qA} \int_{o}^{V_P} C \, dv$$

where $q = 1.6 \times 10^{-19}$ coulombs, A is the diode area, C the capacitance and V the voltage. The doping is also obtained as a function of distance via differential capacitance as in Figure 17. The aluminum is then stripped off in dilute HF which does not etch gallium arsenide. Rechecking has shown that the sample is not changed by this procedure.

Preliminary Experimental Results

Since the preliminary experiment was discussed in the first quarterly report, only the results will be given here for completeness.

The irradiations were performed at the University of California (Berkeley) Reactor using 3 Mev neutrons.

Low energy neutrons were shielded out although no information is available on the energy spectrum nor concerning the presence of other types of radiation.

Toward locating the point where complete compensation just occurs, we obtain:
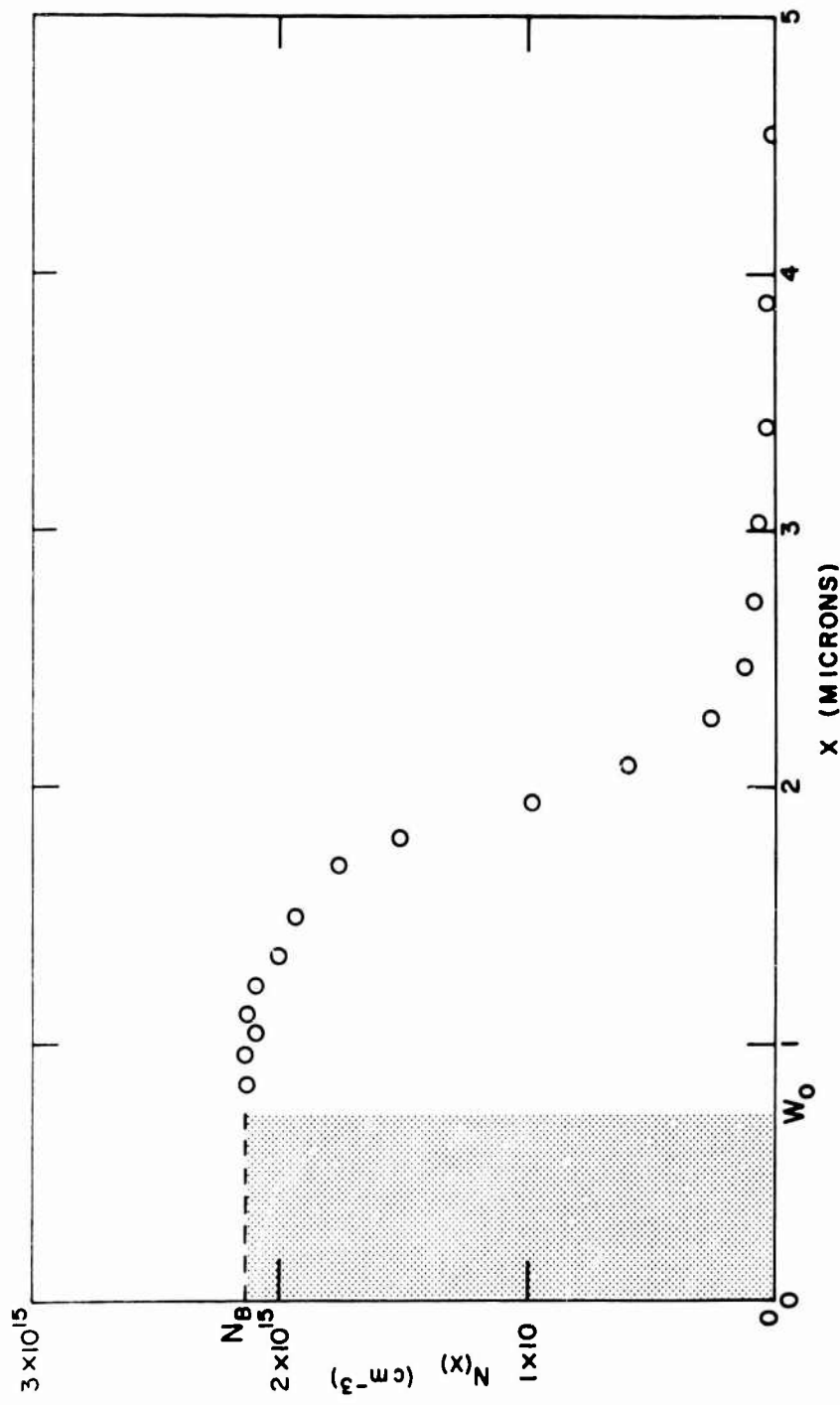
32

Figure 17. Carrier Concentration versus Distance for a Typical Gallium Arsenide Epitaxial Film Determined by Schottky Barrier Differential Capacitance Techniques. (The shaded area shows the extent of the surface depletion layer.)

33

1. Dose = 6.7×10^{13} nvt; 3.8×10^{14} cm^{-3} is completely compensated where 1.3×10^{15} cm^{-3} is not,

2. Dose = 2.3×10^{14} nvt; 4.1×10^{14} cm^{-3} is completely compensated and 3.2×10^{15} cm^{-3} is not, and

3. Dose = 1.5×10^{15} nvt; 6.0×10^{15} cm^{-3} is completely compensated and 5.0×10^{16} cm^{-3} is not.

Compensated samples tend toward intrinsic and no sign of a shift to p-type is detected. The carrier removal rate, $\Delta N/$Dose, is 6 to 10cm^{-1} in accord with the value of 8cm^{-1} given by Aukerman, Davis, Graft and Shilliday.[24] A pronounced tendency for capacitance to decrease with time at a given bias (drift) is noted in many samples and the Hall effect provides the most stable and consistent data.

Only room temperature Hall data were taken so that mobility changes could not be correlated with ionized impurity content. With one exception initial mobilities ranged from 5000 to 8000 cm^2/volt-sec-- in this group all mobilities decreased 10 to 20 per cent. One sample had an anomalously low initial mobility of 2800, which increased after irradiation to 3900 cm^2/volt-sec.

Detailed Material Study

The material study is currently underway so that it is somewhat early to draw conclusions. Furthermore, a few unexpected and unexplained puzzles have developed.

For this study we cut three or four Hall samples from each of four wafers and plan to irradiate repeatedly in small doses until they were fully compensated. Thus fifteen samples have now completed two successive irradiations of 3 Mev neutrons at the Northrup Reactor Facility in Hawthorne, California. The usual attrition due to handling has reduced the number to eleven.

In this set of samples the doping ranges from 0.3 to 1.5×10^{15} cm^{-3} and liquid nitrogen mobilities initially went from 60,000 to 95,000 cm^2/volt-sec. The neutron dosage was from 1.0×10^{13} to 5.0×10^{13} nvt.

One puzzle not yet explained was evident even before irradiation. Previous comparisons of the Hall Q_H and the Schottky barrier Q_{SB} had indicated approximate equality well within $\pm$ 20%. Some of the

34

samples in this study showed a variation of over ± 30%. After irradiation the agreement between the two Q's generally becomes even worse--one sample showing a difference of 50%. After irradiation, the capacitance drift becomes noticeable and the differential capacitance data is often erratic. The Hall data on the other hand remains quite stable and consistent although it is difficult to calculate an average doping from the Hall Q without a dependable knowledge of the effective film thickness. However, the best estimate of carrier removal rate is now 6 to 8 cm^{-1}.

Liquid nitrogen Hall data are also being taken. With some reservations, we assume that the decrease in mobility is due to the increase of ionized impurity content and that the only significant contributors to the L. N. mobility are ionized impurity scattering, μ_I, and polar lattice scattering, $\mu_L = 200,000$ cm^2/volt-sec.[25] Assuming the two types of scattering to be independent, we compute

$$\frac{1}{\mu_I} = \frac{1}{\mu_M} - \frac{1}{\mu_L}$$

where μ_M is the measured mobility. Thus, from μ_I calculated before and after irradiation, ΔN_I, the change in ionized impurity concentration, can be obtained from the Conwell--Weisskopf[26] theory. This kind of analysis yields a reasonably constant value of ΔN_I/Dose = 38 ± 5 cm^{-1}.

Conclusions

While it is rather soon to make decisive statements, the carrier removal rate appears to correlate with earlier work in this field on much higher doped material ($\sim 10^{17} cm^{-3}$) and presumably much less pure material, so that no strong doping concentration dependence is evident. The rate of work is somewhat metered since we are constrained to send the samples away at four to six week intervals. In the final quarter it is expected that the results of the present study will be clear enough to interpret and predict changes in device characteristics.

35

REFERENCES

1. A. S. Grove, "Physics and Technology of Semiconductor Devices," John Wiley and Sons, 1967, p. 311-315.

2. H. Lawrence, R. M. Warner, " Diffused Junction Depletion Layer Calculations," Bell Telephone System, Technical Publications, Monograph 3517, 1960.

3. R. S. C. Cobbold, N. F. Trofimenkoff, "Theory and Application of the Field-Effect Transistor," Proc. IEEE, Vol III, 1964.

4. M. P. Lepselter and S. M. Sze, Bell Sys. Tech. J. $\underline{47}$, 195, 1968.

5. R. A. Zettler and A. M. Cowley, IEEE Trans. Electron Devices $\underline{ED-16}$, 58, 1969.

6. A. Y. C. Yu and E. H. Snow, J. Appl. Phys. $\underline{39}$, 3008, 1968.

7. A. Y. C. Yu and C. A. Mead, Solid-State Electron. (to be published).

8. A. Y. C. Yu and E. H. Snow, Solid-State Electron. $\underline{12}$, 155, 1969.

9. R. A. Aldrich, Paper 8.5 and J. E. Price, Paper 8.6, presented at the 1968 IEEE Int. Electron Devices Meeting, Washington, D. C.

10. W. W. Hooper and W. I. Lehrer, Proc. IEEE (Letters) $\underline{55}$, 1237, 1967.

11. K. E. Drangeid, R. Jaggi, S. Middlehoek, T. Mohr, A. Moser, G. Sasso, R. Sommerhalder and P. Wolf, Electronics Letters $\underline{4}$, 362, 1968.

samples in this study showed a variation of over ± 30%. After irradiation the agreement between the two Q's generally becomes even worse--one sample showing a difference of 50%. After irradiation, the capacitance drift becomes noticeable and the differential capacitance data is often erratic. The Hall data on the other hand remains quite stable and consistent although it is difficult to calculate an average doping from the Hall Q without a dependable knowledge of the effective film thickness. However, the best estimate of carrier removal rate is now 6 to 8 cm^{-1}.

Liquid nitrogen Hall data are also being taken. With some reservations, we assume that the decrease in mobility is due to the increase of ionized impurity content and that the only significant contributors to the L. N. mobility are ionized impurity scattering, μ_I, and polar lattice scattering, $\mu_L = 200,000 \ cm^2/volt\text{-}sec.$ [26] Assuming the two types of scattering to be independent, we compute

$$\frac{1}{\mu_I} = \frac{1}{\mu_M} - \frac{1}{\mu_L}$$

where μ_M is the measured mobility. Thus, from μ_I calculated before and after irradiation, ΔN_I, the change in ionized impurity concentration, can be obtained from the Conwell--Weisskopf[26] theory. This kind of analysis yields a reasonably constant value of $\Delta N_I/Dose = 38 \pm 5 \ cm^{-1}$.

Conclusions

While it is rather soon to make decisive statements, the carrier removal rate appears to correlate with earlier work in this field on much higher doped material ($\sim 10^{17} cm^{-3}$) and presumably much less pure material, so that no strong doping concentration dependence is evident. The rate of work is somewhat metered since we are constrained to send the samples away at four to six week intervals. In the final quarter it is expected that the results of the present study will be clear enough to interpret and predict changes in device characteristics.

REFERENCES

1. A. S. Grove, "Physics and Technology of Semiconductor Devices," John Wiley and Sons, 1967, p. 311-315.

2. H. Lawrence, R. M. Warner, "Diffused Junction Depletion Layer Calculations," Bell Telephone System, Technical Publications, Monograph 3517, 1960.

3. R. S. C. Cobbold, N. F. Trofimenkoff, "Theory and Application of the Field-Effect Transistor," Proc. IEEE, Vol III, 1964.

4. M. P. Lepselter and S. M. Sze, Bell Sys. Tech. J. 47, 195, 1968.

5. R. A. Zettler and A. M. Cowley, IEEE Trans. Electron Devices ED-16, 58, 1969.

6. A. Y. C. Yu and E. H. Snow, J. Appl. Phys. 39, 3008, 1968.

7. A. Y. C. Yu and C. A. Mead, Solid-State Electron. (to be published).

8. A. Y. C. Yu and E. H. Snow, Solid-State Electron. 12, 155, 1969.

9. R. A. Aldrich, Paper 8.5 and J. E. Price, Paper 8.6, presented at the 1968 IEEE Int. Electron Devices Meeting, Washington, D. C.

10. W. W. Hooper and W. I. Lehrer, Proc. IEEE (Letters) 55, 1237, 1967.

11. K. E. Drangeid, R. Jaggi, S. Middlehoek, T. Mohr, A. Moser, G. Sasso, R. Sommerhalder and P. Wolf, Electronics Letters 4, 362, 1968.

12. H. Statz and W. V. Munch, Solid-State Electron. 12, 111, 1969.

13. R. A. Aldrich and A. Y. C. Yu, Electronics (to be published).

14. D. K. Wilson et al., Final Contract AF19(628)-4157, 1967.

15. H. S. Les and S. M. Sze, Paper presented at IEEE Semi-conductor Interface Specialists Conf., Las Vegas, Nevada, 1968.

16. E. H. Snow, A. S. Grove and D. J. Fitzgerald, Proc. IEEE 55, 1168, 1967.

17. D. J. Fitzgerald and E. H. Snow, IEEE Trans. Electron Devices ED-15, 160, 1968.

18. D. J. Fitzgerald and A. S. Grove, Proc. IEEE (Letters) 54, 1601, 1966.

19. A. S. Grove and D. J. Fitzgerald, IEEE Trans. Electron Devices ED-12, 619, 1965.

20. H. J. Stein, Sandia Reports SC-R-65-938, 1965, and SC-R-64-193, 1964.

21. L. J. Van der Pauw, "A Method of Measuring Specific Resistivity and Hall Effect of Discs of Arbitrary Shape," Philips Research Reports 13, 1, Feb. 1958.

22. W. W. Hooper, B. R. Cairns, et al., "Feasibility of a GaAs Schottky Barrier Gate FET," Tech. Rept. AFAL-TR-69-30, Feb. 1969.

23. C. A. Mead, "Metal-Semiconductor Surface Barriers," Solid-State Electronics 9, 1023, 1966.

24. L. W. Aukerman, P. W. Davis, R. D. Graft and T. S. Shilliday, "Radiation Effects in GaAs," JAP 34, 3590, Dec. 1963.

25.   D. E. Bolger, J. Franks, J. Gordon and J. Whitaker,
        "Preparation and Characteristics of Gallium Arsenide,
        Proceedings of the International Symposium on Gallium
        Arsenide, Reading, England, 1966, p. 16, Institute of
        Physics and the Physical Society of London, 1967.

26.   E. Conwell and V. F. Weisskopf, "Theory of Impurity Scattering
        in Semiconductors, " Phys. Rev. $\underline{77}$, 388, Feb. 1950.

DOCUMENT CONTROL DATA - R & D

(Security classification of title, body of abstract and indexing annotation must be entered when the overall report is classified)

1 ORIGINATING ACTIVITY (Corporate author)	2a. REPORT SECURITY CLASSIFICATION
Fairchild Semiconductor, a Division of Fairchild Camera and Instrument Corporation	UNCLASSIFIED
464 Ellis Street, Mt. View, California 94040	2b. GROUP

3 REPORT TITLE

STUDY OF RADIATION EFFECTS ON NOVEL SEMICONDUCTOR DEVICES

4 DESCRIPTIVE NOTES (Type of report and inclusive dates)
Scientific   Interim

5 AUTHOR(S) (First name, middle initial, last name)

Edward H. Snow   Heinz-Peter Albus

Douglas A. Tremere   Albert Y. C. Yu

6 REPORT DATE	7a. TOTAL NO. OF PAGES	7b. NO. OF REFS
June 1969	47	26

8a. CONTRACT OR GRANT NO.	9a. ORIGINATOR'S REPORT NUMBER(S)
F19628-69-C-0118	
b. Project, Task, Work Unit Nos.	Scientific Report No. 1
4608-05-01	
c. DoD Element: 62403F	9b. OTHER REPORT NO(S) (Any other numbers that may be assigned this report)
d. DoD Subelement: 634608	AFCRL-69-0259

10 DISTRIBUTION STATEMENT No. 1
Distribution of this document is unlimited. It may be released to the clearing-house, Department of Commerce, for sale to the general public.

11 SUPPLEMENTARY NOTES	12 Air Force Cambridge Research
TECH, OTHER	Laboratories (CRW) L. G. Hanscom Field Bedford, Massachusetts 01730

13 ABSTRACT

A radiation resistant power JFET has been designed to have an I_{DSS} of 4 amps, a pinch-off voltage of 8 volts and a breakdown voltage of 40 volts. The predicted change in I_{DSS} or G_m for this device after 10^{15} nvt is about 36%. Following this design, several runs of devices have been fabricated and characterized. Outstanding problems include high pinch-off voltages (probably due to the graded nature of the gate junctions), low I_{DSS} (probably due to source and drain series resistance), and low breakdown voltage (due to epitaxial defects in the large area bottom gate). The best results to date are I_{DSS} = 2.5 amp with a pinch-off voltage of 12 volts.

Several types of silicon planar Schottky barrier diodes have been exposed to ionizing radiation and the same phenomena are observed as on p-n junctions - increase in the fast surface state density and the build-up of a positive space charge in the oxide. These cause excess currents in the forward direction and "soft" reverse characteristics. Aluminum diodes are relatively less affected by radiation than platinum diodes because of the lower barrier height and higher thermionic emission current of the former. The barrier height itself does not change with radiation.

Capacitance-voltage and Hall effect measurements have been made on high quality epitaxial GaAs before and after exposure to nuclear reactor radiation. From changes in carrier concentration, a neutron carrier removal rate of 6 to 8 cm^{-1} has been determined. From changes in liquid nitrogen mobility (and some assumptions on scattering mechanisms), an introduction rate for ionized scattering centers of 38 ± 5 cm^{-1} has been determined.

DD FORM 1473 NOV 65
REPLACES DD FORM 1473, 1 JAN 64, WHICH IS OBSOLETE FOR ARMY USE.

14 KEY WORDS	LINK A		LINK B		LINK C	
	ROLE	WT	ROLE	WT	ROLE	WT
Field Effect Transistor						
Power Device						
Radiation Resistant						
Schottky Barrier						
Neutron Radiation						
Ionizing Radiation						
GaAs						
Carrier Removal						